# Utilization of Space-Based TDoA and FDoA for Cislunar Orbit Determination

**Michael R. Thompson, Matthew D. Popplewell, Bradley Cheetham**
*Advanced Space, LLC*

## ABSTRACT

This study evaluates the potential observability benefits of space-based passive RF systems compared to other ground-based and space-based observers for cislunar Space Domain Awareness. TDoA and FDoA observations are used for orbit determination of objects in the lunar vicinity using observers in GEO and XGEO. The results are compared to ground-based observations in order to analyze the performance gains over existing architectures. Results show using space-based systems result in faster filter convergence and more accurate state estimates.

## 1. INTRODUCTION

Over the past decade, the space industry has seen a renewed interest in new space missions about the Moon and in cislunar space. Already several organizations have placed vehicles in cislunar space such as NASA's Lunar Reconnaissance Orbiter in 2009 and China's Chang'e-5 in 2020. Furthermore, NASA's Artemis program aims to enable the return of humans to the Moon by 2024 with plans for supporting space architecture, such as the Lunar Gateway. As the number of space objects in cislunar space increases, so too does the need for an improved understanding of how to reliably track such objects. Current Space Domain Awareness (SDA) capabilities are primarily concerned with Earth-centered objects. The European Space Agency (ESA) estimates about 31,450 debris objects tracked by the Space Surveillance Network (SSN) [1]. However, the existing ground-based architecture is ill-suited for growing operations in the cislunar domain. Complex nonlinear dynamics, body occultations, lunar exclusions, poor geometric observability, and low signal-to-noise ratio (SNR) observations complicate cislunar SDA [2]. A potential alternative is employing space-based platforms to supplement or replace ground-based platforms. Prior work has demonstrated the ability to perform orbit determination (OD) via optical measurements between two cislunar spacecraft [3]. This study expands this analysis to the utilization of time difference of arrival (TDoA) and frequency difference of arrival (FDoA) measurements.

Using ground-based receivers for orbit determination of cooperative spacecraft transmitting radio frequency (RF) signals has been employed for several decades. Ground stations have access to stable timing sources and can yield large baselines with stations separated by thousands of kilometers, resulting in precise measurements. The Deep Space Network's (DSN) delta-differential one-way ranging (ΔDOR), which uses measurements of both the spacecraft and quasars to calibrate for instantaneous atmospheric conditions and provide plane-of-sky information, can produce measurements as low as single digit nanoradians. Assuming the downlink signal strength is adequate, TDoA and FDoA can also be used with non-cooperative spacecraft.

In domains where the use of ground-based platforms are stressed, the use of space-based TDoA and FDoA observations of an RF-emitting resident space object (RSO) can supplement ground systems. Passive RF systems do not have the exclusion constraints of optical systems or the power requirements of active radar systems. Additionally, the TDoA and FDoA OD methodology can be used to estimate the state of almost any transmitting RSO, with no special downlink radio configurations required.

This study demonstrates the observability performance of space-based TDoA and FDoA observations of RF-emitting RSOs in cislunar space. Orbit determination of spacecraft in the lunar vicinity using TDoA and FDoA is performed by observers in GEO and cislunar orbits. Measurements are simulated in a high-fidelity dynamical environment and orbit determination setup for multiple cases.

## 2. XDA ARCHITECTURE

Existing literature on cislunar SSA encompasses a wide range of concepts. Previous analyses focus on areas such as trajectory design, sensor tasking, data processing, and filter modeling with scopes varying between addressing the full cislunar domain or some subset, such as L1 Lagrange point orbits. This section will explore previous space-based

cislunar tracking concepts with a focus on the placement and operation of observer platforms. Space-based observers have previously been studied in orbits about the Earth, Lagrange points, and the Moon.

Platforms in traditional Earth-centered orbits offer minimal advantage over Earth ground-based observers for cislunar SSA as they are still plagued by extreme distances, lunar and solar exclusion angles, and insufficient geometric diversity. Knister et al. determined ground-based observers are incapable of observing an L1 Lyapunov orbit due to lunar exclusion angles, but a LEO constellation can view the spacecraft "when the Earth blocks the Moon from the sensor field of view". The authors deliver a LEO architecture that has improved performance over ground systems but ultimately recommend future study of observers in Lagrange and Moon-centered orbits [4]. Fowler et al. use an observer in an elliptical, inclined Medium Earth Orbit (MEO) to observe spacecraft in L1 and L2 Lyapunov orbits. The results show the Earth-centered spacecraft is only capable of observing the Lyapunov orbits for about 65% of the time. Additionally, the performance of the observation platform is unsatisfactory as a result of the vast distances between the observer and target spacecraft. The author recommends placing observing spacecraft in Moon-centered or Lagrange point orbits for cislunar SDA [5].

To combat the challenges for cislunar SDA, several authors have proposed placing observers in Lagrange point and cislunar orbits. Doing so reduces the range between observer and target, improves the geometric diversity of observations, and potentially reduces exclusions and occultations. Hill developed Linked, Autonomous, Interplanetary Satellite Orbit Navigation (LiAISON), which uses peer-to-peer space-based tracking for cooperative orbit determination and navigation and has applied it to multiple applications in cislunar space [6]. While originally developed for cooperative orbit determination and navigation, in the years since authors have extended the co-estimation methodology to include optical measurements, and the concept could easily be applied to the problem of cislunar SDA [7]. Vendl and Holzinger have studied the cislunar SDA capabilities of periodic libration point orbits with results showing resonant retrograde periodic orbits are favorable for RSO observation. Specifically, the authors present resonant L1 and L2 Lyapunov orbits that, when phased correctly, have favorable solar geometry and near-continuous observation of the cislunar region [8]. Gupta et al. have examined resonant orbits in the circular restricted three-body problem (CR3BP) and found a 2:1 retrograde resonant orbit can provide long-term full observation of cislunar space. Furthermore, such an orbit has a periapsis near GEO and an apoapsis in the lunar vicinity, allowing access to both the Earth and Moon [9]. Frueh et al. expands this analysis to further refine the orbit of interest for cislunar SDA and investigate the necessary orbit maintenance and determination. The authors present a 2:1 retrograde resonant orbit that travels between GEO and the Moon in one revolution and traverses all of cislunar space in 20 revolutions [10].

Observers in Moon-centered orbits offer similar benefits to those in libration point orbits. Fowler et al. compare a spacecraft in an elliptical, inclined MEO to a Moon orbiter for observing L1 and L2 Lyapunov orbits. While no orbital information is given about the Moon orbiter, the authors present that the lunar spacecraft has considerable observability improvement over the Earth spacecraft: the L1 orbiter is unavailable for observation by the Moon orbiter for 20% of the time compared to 65% of the time for the Earth observer. Furthermore, the Moon observations provide greater geometric diversity due to the reduced range [5].

## 3. VERY LONG BASELINE INTERFEROMETRY

Very long baseline interferometry (VLBI) is a technique originally from radio astronomy and geodesy that utilizes antennas separated by large distances to study RF sources [11]. By correlating the received signals at two or more antennas, the time difference of arrival (TDoA) of the signal can be computed. By basic geometry, this TDoA measurement provides angular information in the plane defined by the RF source and the two receiving antennas. This geometry is shown in Fig. 1. In this figure, the TDoA is represented by $\tau$, and the leg of the triangle representing the TDoA has a length of $\tau$ multiplied by the speed of light. As seen in this figure, with the TDoA and a knowledge of the baseline length between the two receivers, there is angular information gained in the plane of the two receivers and the transmitter.

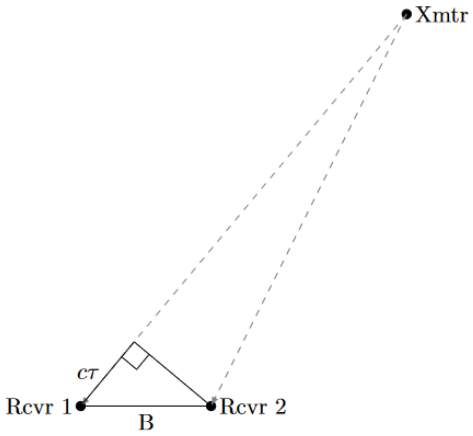


Fig. 1: Geometry formed by two receivers and one transmitter.

VLBI-based techniques are extremely useful for cooperative deep space navigation. The primary radiometric measurements typically used for deep space navigation are ranging and Doppler, which provide information along the line-of-sight direction. The addition of precise angular information can provide large improvements in orbit determination accuracy.

For the Deep Space Network, the primary VLBI-based technique is delta differential one-way ranging (ΔDOR). In ΔDOR, the cooperative spacecraft transmits several large bandwidth ranging tones which are received by two ground stations at different complexes simultaneously. The ranging tones emitted from the spacecraft have several inherent errors and biases based on spacecraft clock offsets and frequency stability. A differential one-way range measurement (DOR) can be computed by differencing the one-way range measurements at each station where the signal is received. This differential removes spacecraft-side errors (such as onboard clock errors) since these errors affect the observed signal at both stations. The *delta* in ΔDOR is an additional differential between the received spacecraft signal and the signal of a nearby (in angular space) RF source with known properties, usually a quasar. This additional differential removes errors on the receiver side such as media delays clock offsets, and earth orientation because the receiver-side delays affect both the spacecraft signal and quasar signal [12], [13]. By 2004, DSN ΔDOR measurement errors were conservatively budgeted at 0.06 ns (corresponding to 2.25 nRad of angle on an 8,000 km baseline), and observed residuals were on the order of 0.03 ns (1-sigma) [12].

There are more complicated phase-matching methods that utilize many baselines simultaneously to resolve phase ambiguities, but for the purposes of this study, only one-baseline configurations will be analyzed [12].

From Moyer [14], the time difference of arrival (wideband interferometry in DSN parlance) is calculated as:

$$IWS\ (ns) = -\frac{[(\varphi_2 - \varphi_1)_B - (\varphi_2 - \varphi_1)_A]_{fractional\ portion}}{\omega_B - \omega_A} * 10^9$$

In this equation, the phase of two simultaneously transmitted frequencies is measured at two different locations. The transmitted frequencies are given as $\omega_B$ and $\omega_A$, where $\omega_B > \omega_A$. For the numerator of this equation, the "fractional portion" subscript represents a modulo calculation – the integer number of cycle differences is discarded, and only the fractional portion remains. This formulation is mathematically equivalent to the difference in one-way light time from a spacecraft to two stations with synchronized clocks, or TDoA. Note that in this formulation, the definition assumes two transmitted frequencies, preferably with a wide bandwidth such that $\omega_B - \omega_A \gg 0\ Hz$. Via the use of mathematical correlators, it is possible to capture a wideband recording without two distinct frequency tones and compute a time difference of arrival based on a carrier alone, or weak / near side-bands (see for example the work of Kratos or other passive-RF providers) [15]–[18]. With small bandwidths such as a carrier alone, TDoA measurements are typically less accurate than a spacecraft transmitting distinct tones, but measurement generation is still possible.

Again from Moyer [14], the frequency difference of arrival (narrowband interferometry in DSN parlance) is calculated as:

$$INS\ (Hz) = \frac{-1}{T_c}[(\varphi_2 - \varphi_1)_e - (\varphi_2 - \varphi_1)_s]$$

In this equation, the difference in carrier phase between receiver 1 and receiver 2 is differenced at the start and end time of some count interval $T_c$.

The performance of VLBI-based techniques is well-studied for cooperative spacecraft that transmit DOR tones specifically for the purpose of ground-based VLBI [17], [19]–[25]. Given the high-level SDA-centric goals of this research, the authors are particularly interested in simulating realistic TDoA and FDoA noises for targets with very narrow bandwidths, and not requiring dedicated DOR tones. A small summary of observed and simulated performances in the literature for these such cases is given in Table 1.

Table 1: Narrow bandwidth TDoA/FDoA performance without DOR tones.

| Author | Network | Target | Simulated/Real | TDoA Noise (1-sigma) | FDoA Noise (1-sigma) |
|---|---|---|---|---|---|
| Kaliuzhnyi et al. [26] | Ukraine / Latvia | GEO | Real | 8.7 ns | - |
| Huang et al. [18] | CVN | GEO | Real | 3.6 ns | |
| Kinzley et al. [27] | Simulated Global | EM L1 | Simulated | 20 ns | 0.04 Hz |
| Zheng et al. [21] | CVN | Lunar (CE-1) | Real | < 5.5 ns | - |
| Zheng et al. [21] | CVN | Lunar (CE-2) | Real | ~4-5 ns | - |
| Geeraert and McMahon [28], [29] | Simulated | Simulated | Simulated | 35 ns | 0.2 mHz |

Note that while some authors in the literature include integration/averaging times in their publications, many do not, which makes perfect replication difficult. For the purpose of this study, the values from Kinzley et al. will be utilized along with a 5-minute measurement cadence.

## 4. BENEFITS OF SPACE-BASED PLATFORMS

As previously discussed, TDoA provides angular information in the plane that is formed by the transmitting spacecraft and the two receivers. For the typical case of a very high-altitude spacecraft and two ground-based receivers, this plane primarily rotates with the rotation of the Earth, but the normal vector of the plane remains close to constant – any motion in the normal vector of the plane is primarily driven by the motion of the transmitter. If the receivers have significant out-of-plane motion, the plane in which information is collected changes over time, which allows for better observability and quicker convergence. A clear method of obtaining this out-of-plane motion is via space-based receivers.

In addition to observability benefits of space-based receivers, another clear benefit is that space-based receivers can gather measurements with significantly longer baselines than ground-based receivers. Revisiting the fundamental geometry of the problem in Fig. 1, the angle between the baseline vector and the transmitter can be expressed as $\cos^{-1}(\frac{c\tau}{B})$. Differentiating with respect to the time delay measurement, the partial derivative is inversely proportional to the length of the baseline. Practically what this means is that for a given measurement accuracy, longer baselines translate into better angular resolutions, which is one of the reasons why there has been continued interest in space-based VLBI techniques from astronomers [30]–[32].

To demonstrate the observability and information content benefits, a dilution of precision (DOP) metric is compared for two ground-based receivers and two receivers in GEO. This DOP formulation is based on the work of Bard and Ham, and was recently demonstrated for ground-based TDoA networks for tracking launch vehicles or spacecraft by Marzioli, Santoni, and Piergentili [33], [34]. The difference from these previous formulations is that the previous

literature computed a DOP based on multiple simultaneous measurements (i.e. a network of ground receivers). The analysis in this work is based on an estimation paradigm where there are only two receivers at a time, and as such, some of the matrix inverse calculations utilized in the previous literature encounter singularity issues. To still produce meaningful results, a matrix pseudo-inverse is taken instead. The DOP metric produces a purely geometry-based view of the observability of the TDoA problem.

$$H = \left[\frac{\partial \Delta t}{\partial x}\right]$$

$$\frac{\partial \Delta t}{\partial x} = \frac{x_T - x_i}{\|x_T - x_i\|} - \frac{x_T}{\|x_T\|}$$

$$DOP = \sqrt{trace(H^T H)^{-1}}$$

In this formulation, $x_T$ represents the state of the transmitter with respect to the reference receiver, and $x_i$ represents the state of the second receiver with respect to the reference receiver (although it could scale to multiple receivers as in the original implementation). Again, in the case of two receivers, $H^T H$ produces a singular matrix, so singular value decomposition is utilized to solve the pseudo-inverse.

The DOP metric over time is shown in Fig. 2 for a transmitter in an Earth-Moon L2 halo orbit, two ground-based receivers on Mauna Kea and Owens Valley, CA, and two space-based receivers in GEO at 130 and 170 degrees longitude. In terms of longitude, the two pairs of receivers are roughly equally spaced, but the GEO satellites clearly yield a much larger baseline, and yield DOP values roughly an order of magnitude lower than the ground-based receivers. Approximately twice per month the DOP of the GEO pair will experience very short-period spikes as the Moon crosses the equatorial plane. This is caused by the transmitter and two GEO receivers becoming very close to colinear, which leads to poor geometric observability.

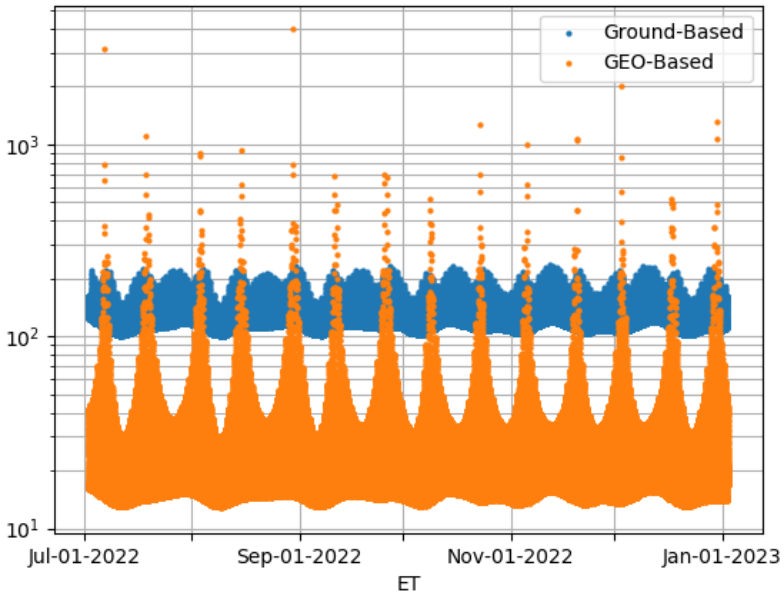


Fig. 2: DOP of two ground-based and space-based receivers for a transmitter near Earth-Moon L2.

While there are clear benefits of using space-based VLBI assets instead of or in conjunction with Earth-based assets, there are also clear challenges. Wideband RF recordings can be extremely data intensive, which is challenging for radiation-hardened and space-qualified hardware. For the Spektr-R mission launched in 2011, one of two dedicated in-space VLBI platforms that have been demonstrated, the ground data processing center regularly processed 100-800 GB per hour of RF recordings per antenna for ground-based dishes, but the space segment was limited by a 144 Mbit/s

downlink [35]. A recent white paper in support of the 2020 Decadal review for a space-based VLBI platform at the Sun-Earth L2 Lagrange point budgeted on the order of 230 TB of data per 6-hour observation [32]. These are extreme data volume constraints, particularly for a CONOP where the data must be downlinked to the ground for correlation. Another challenge, albeit less significant than the data volume challenge, is the challenge of orbit determination. Ground-based VLBI installations are often known to centimeter-level precision given their use in geodesy. Such accuracy is typically unachievable for spacecraft. A potential mitigation of orbit determination challenges for space-based platforms, however, is the utilization of the VLBI observables themselves to approximate their own state. This was an experimental technique that was demonstrated on Spektr-R, which saw improvements in orbit determination uncertainty of approximately an order of magnitude over ranging and Doppler alone by utilizing the VLBI observations of known radio sources in the ground-based orbit determination engine [36]. It is unknown whether such a technique could be applied with the narrow bandwidths and position uncertainties of SDA targets, but given the prior work of Greaves and Scheeres on co-estimation based on non-cooperative optical measurements, it is plausible that the estimation theory of the technique may translate to the problem of SDA [7]. Finally, one of the last major constraints on space-based VLBI systems is the accuracy of onboard clocks. Historically, there were relatively few options for very stable onboard clocks. Spektr-R was the first science mission to launch with an active H-maser onboard and the JAXA VSOP mission kept timing stability via a phased locked loop with a stable timing source on the ground during VLBI measurements [30]. While neither of these options are truly ideal for flexible platforms and CONOPS, the Spektr-R and VSOP missions do demonstrate that there are feasible options for maintaining the necessary levels of clock stability for space-based VLBI platforms. Depending on the integration time requirements for measurements and desired coverage of frequency bands, a clock of similar performance to the recent Deep Space Atomic clock could be a reasonable SWaP option when compared to an onboard hydrogen maser or two-way lock with the ground [37].

## 5. SIMULATION TESTBED

To test the plausibility of space-based TDoA and FDoA observations for estimating the states of transmitting RSOs near the Moon, a measurement simulation and orbit determination testbed was developed. The three transmitters tested are spacecraft in an Earth-Moon L2 halo, a distant retrograde orbit (DRO), and on a low-energy transfer with an apogee towards the Sun. All three of these transmitters represent potentially stressing cases for some optical sensors – the low-energy transfer due to its long loiter time on the illuminated side of Earth, and the L2 halo and DRO due to their persistent low angular separation from the Moon as viewed from the Earth.

The three pairs of VLBI observers are two ground-based, two in GEO, and two in an Earth-Moon L1 libration point orbit. The ground-based receivers are placed at the location of VLBA sites on Mauna Kea and in Owens Valley, CA, providing a baseline of over 4,000 km. The two GEO spacecraft are stationkept at 130 and 170 deg W. As previously discussed, while this separation is similar to the separation of the two ground-based receivers in terms of longitude, the much higher radius yields a much larger baseline – on the order of 28,000 km. The two receivers in an L1 halo are phased such they are offset by half of the period of the orbit. The effective baseline of these observers varies from 20,000 – 50,000 km. The additional benefit of the L1 halo orbit design is that the baseline formed between the two receivers stays relatively close to perpendicular to RF signals returning from the lunar vicinity to the Earth, avoiding positions where the 3 objects in the VLBI problem are nearly colinear. Additional details on the transmitter and receiver pairs are given in Table 2. Additionally, the trajectories in question are shown in Fig. 3 - Fig. 5.

Table 2: Details of test transmitters and receivers.

| Location | Notes |
|---|---|
| **Transmitter** | |
| Earth-Moon L2 Halo | ~15.09-day period, Northern |
| Distant Retrograde Orbit | ~15.91-day period |
| Low-Energy Transfer | Apogee towards the Sun, based on CAPSTONE transfer [38] |
| **Receiver** | |
| GEO | 130 deg W |
| GEO | 170 deg W |
| Ground-Based Dish | Mauna Kea |
| Ground-Based Dish | Owens Valley, CA |
| Earth-Moon L1 Halo | ~11.94-day period, Northern |
| Earth-Moon L1 Halo | ~11.94-day period, Northern, offset by half period in phase |

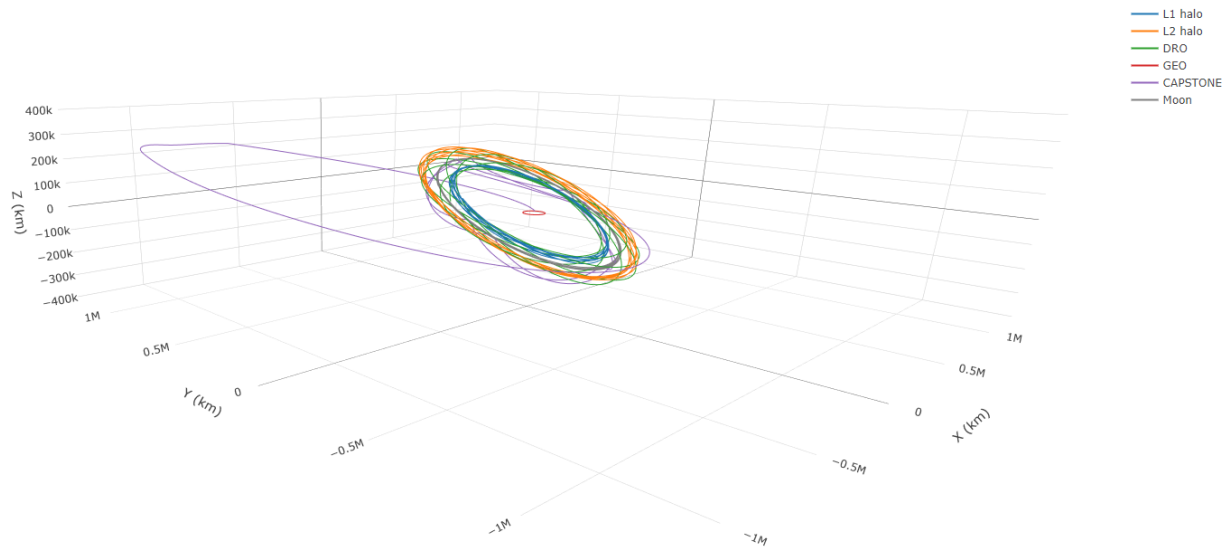


Fig. 3: Transmitter and receiver orbits in Earth-centered inertial frame.

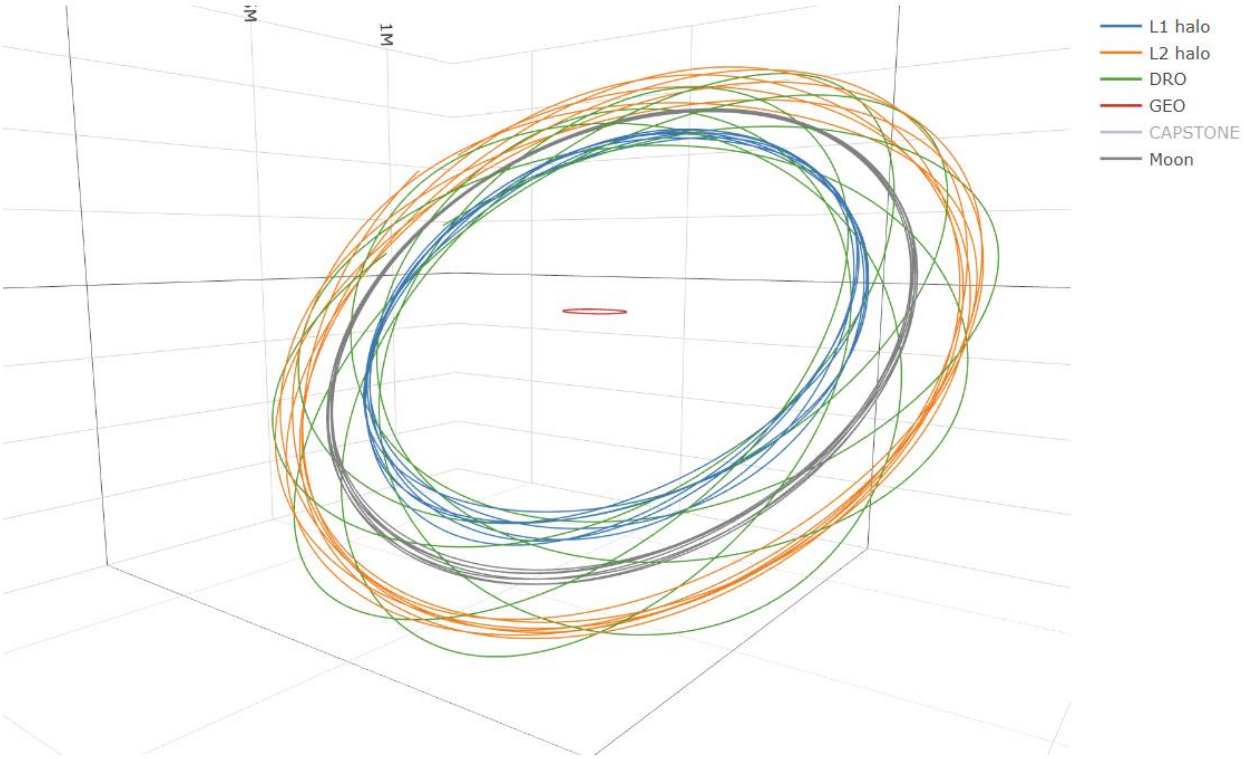

Fig. 4: Transmitter and receiver orbits in Earth-centered inertial frame with CAPSTONE removed.

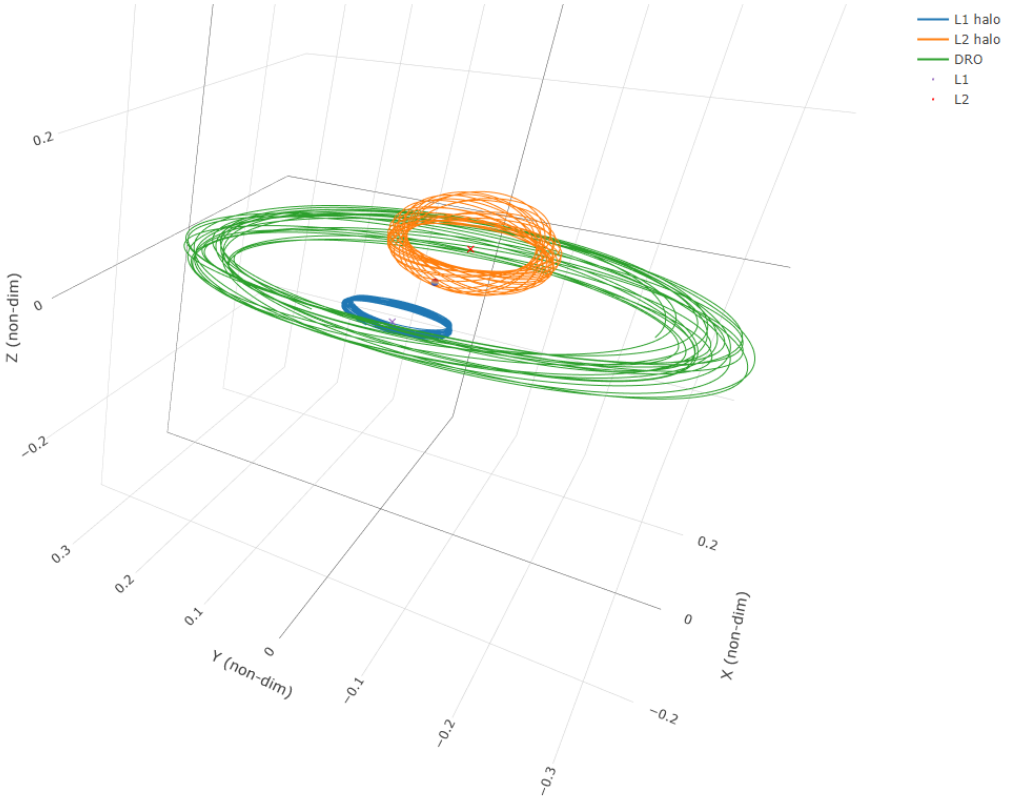


Fig. 5: Halo and distant retrograde orbits in Earth-Moon rotating frame.

The simulated measurements in this study utilize the noise values provided by Kinzly et al. and are detailed in Table 3 [27]. The measurement noise values from these authors fall into the same order of magnitude as demonstrated experimentally by other authors with narrow bandwidth VLBI measurements that are typical of SDA applications. The measurement simulation testbed applies standard measurement elevation angle and occultation constraints based on both the Earth and Moon.

Table 3: Measurement simulation parameters.

| Data Type | Cadence | Noise (1-sigma) |
|---|---|---|
| TDoA | 300 sec | 20 ns |
| FDoA | 300 sec | 0.04 Hz |

## 6. SIMULATED RESULTS

Simulated orbit determinations were performed based on the transmitter/receivers and measurement specifications given above. All orbit determinations are performed in a full ephemeris model in an operations-like setup utilized for XDA studies and operations at Advanced Space. For all cases, the filter is initialized with an a priori uncertainty (1-sigma) of 1,000 km and 100 m/s in each Cartesian direction. Results and discussion for each transmitter / receiver case is given below.

### L2 Transmitter

The first case examined is the case of a transmitter in an Earth-Moon L2 halo orbit. This represents a trajectory that remains persistently at a low angular separation from the Moon as viewed from Earth, making optical observations

difficult. The 3-sigma covariances in position and velocity for 1 revolution of ~ 15 days are shown in Fig. 6 and Fig. 7.

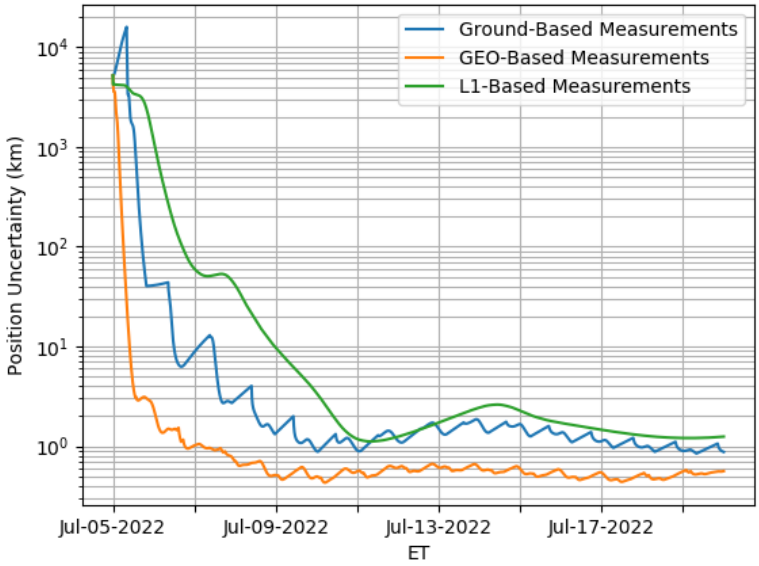


Fig. 6: Estimated position uncertainty (3-sigma) of L2 halo transmitter.

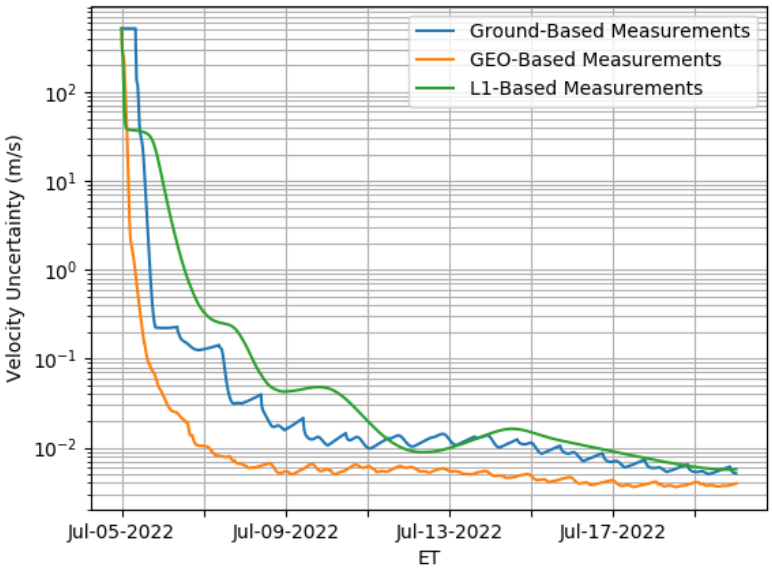


Fig. 7: Estimated velocity uncertainty (3-sigma) of L2 halo transmitter.

An immediately clear trend in estimating the state of the L2 halo transmitter is that the pair of GEO receivers provides the most accurate estimate, with 3-sigma covariances below 1 km and 1 cm/s. Additionally, the pair of GEO receivers provides the fastest convergence to a steady state solution, converging in approximately 2.5 days. These receivers outperform the ground-based receivers, an expected result given the larger effective baseline and superior viewing geometry.

A less-expected result is the relatively poor performance of the two observers in an L1 halo orbit. Despite remaining close to perpendicular to the Earth – L2 line, which should provide very good TDoA/FDoA observability, the two L1 observers tend to perform slightly worse than both the ground-based receivers and GEO receivers. Additionally, the solutions produced by the L1 observers converges to the steady-state at roughly the same rate as the ground-based observers, and slower than the GEO observers.

It is very possible that the short period viewing geometry changes of the GEO observers are better suited to fast convergence than the long period relative geometry changes between two observers in L1 and a transmitter in L2. When a similar previous study was performed based on simulated space-based optical data, the convergence rates were observed to be on the order of half of a period to a full period [3]. These convergence rates have been replicated by other authors since in similar applications [27]. In this TDoA/FDoA study, similar convergence rates are seen for the ground-based and L1-based observers, but the GEO-based observers converge much faster. This is an interesting finding that may be applicable to other data types as well and should be further explored in future work.

**DRO Transmitter**

The second case examined is the case of a spacecraft in a distant retrograde orbit (DRO). DROs are families of orbits which are very stable. If properly injected, RSOs can remain here for decades or longer. The exact angular separation will depend on the specific DRO, but typically DROs will remain within 15-20 degrees of the Moon as viewed from the Earth, again making optical observations difficult for some optical platforms. The 3-sigma covariances in position and velocity for 2 revolutions of this DRO are shown in Fig. 8 and Fig. 9.

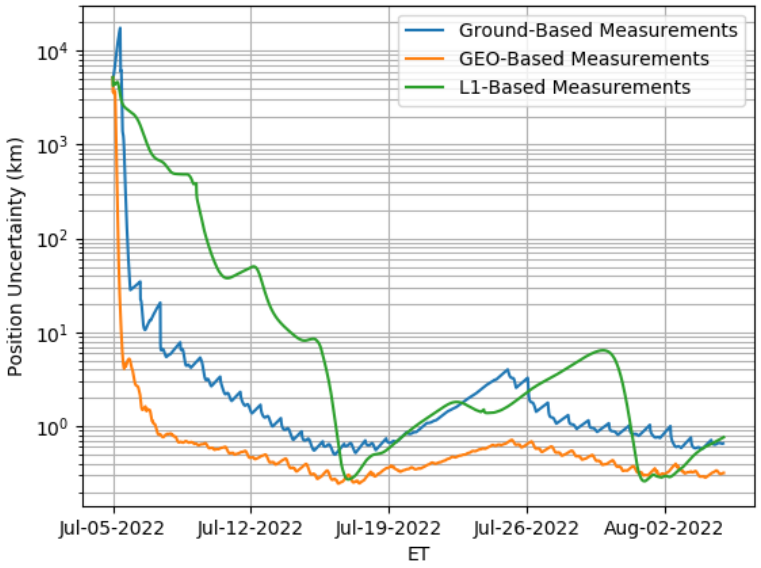


Fig. 8: Estimated position uncertainty (3-sigma) of DRO transmitter.

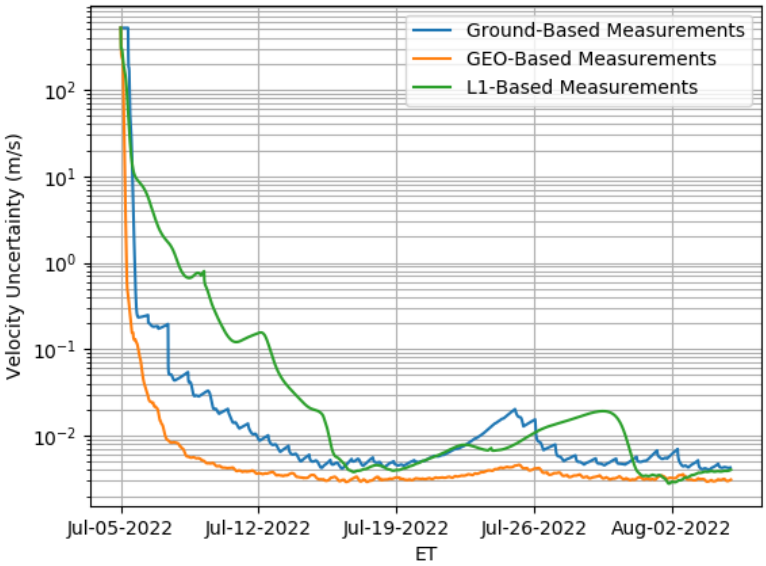


Fig. 9: Estimated velocity uncertainty (3-sigma) of DRO transmitter.

The results shown for the DRO transmitter case are similar to the results seen for the transmitter in L2. The GEO-based receivers still obtain the most accurate solution. However, there are some features in the data that are worth further exploration. After approximately 1 full revolution, all 3 observers experience approximately 1 week where the state uncertainty rises despite the measurements being gathered. This usually occurs due to the underlying dynamics of the system or due to low observability. The section of the DRO being estimated during this rise in the state uncertainty is shown in red in Fig. 10.

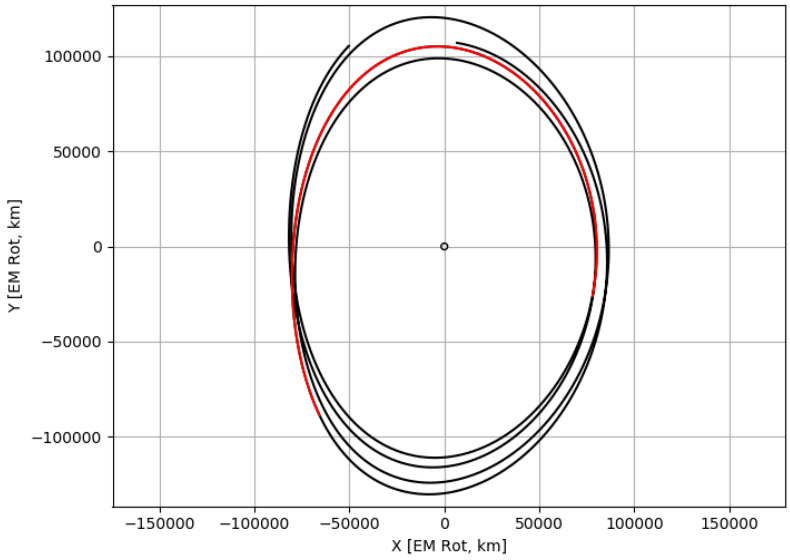


Fig. 10: DRO shown in the Earth-Moon Rotating XY plane. The section where the underlying state uncertainty rises for all cases is highlighted in red.

Additionally, there is some irregular behavior in the state uncertainties from the pair of L1 observers, however this can be attributed to their unique geometry with respect to the DRO. As seen in Fig. 5, the L1 halo orbit resides inside the DRO as viewed in the Earth-Moon rotating frame. Due to this geometry, the pair of L1 observers have a relatively

close approach with the DRO transmitter once per orbit, which corresponds with a large decrease in the estimated state uncertainty. Due the directionality of RF transmissions and the relatively fast angular rates, measurements during this portion of the orbit may not be feasible in an actual system, but the mathematical benefits are clearly seen in this study.

**Low-Energy Transfer Transmitter**

The last case examined in this study is of a low-energy transfer based on the trajectory of CAPSTONE, which is currently en route towards the Moon [38]. The apogee of this transfer is approximately 1.5 million km from Earth, and of note to SDA systems, the apogee is on the illuminated side of the Earth, making optical observations not feasible. The case studied here simulates the first two months of this transfer and goes through apogee. Additionally, given that it is based on the CAPSTONE trajectory, the data arc runs through a deterministic maneuver near apogee. This requires solving for the maneuver in the filter, which can easily be seen in the filter covariance. The 3-sigma covariances in position and velocity for the first two months of this transfer are shown in Fig. 11 and Fig. 12.

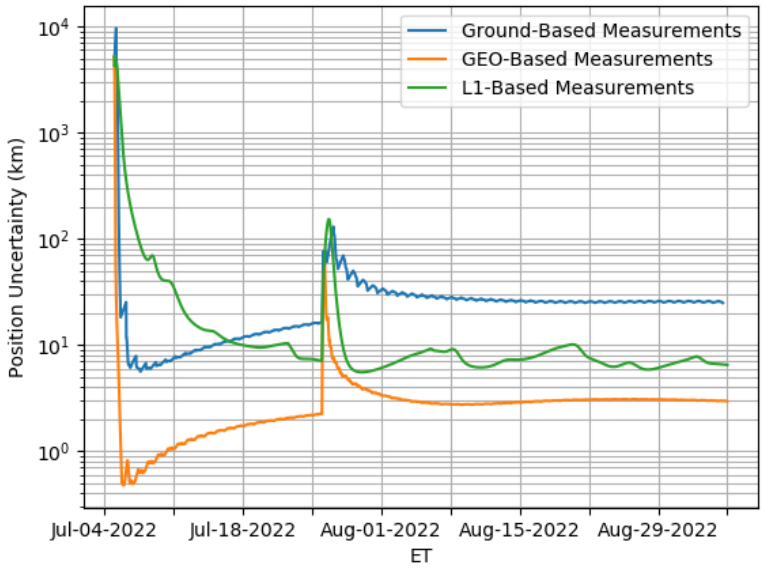


Fig. 11: Estimated position uncertainty (3-sigma) low-energy transfer transmitter.

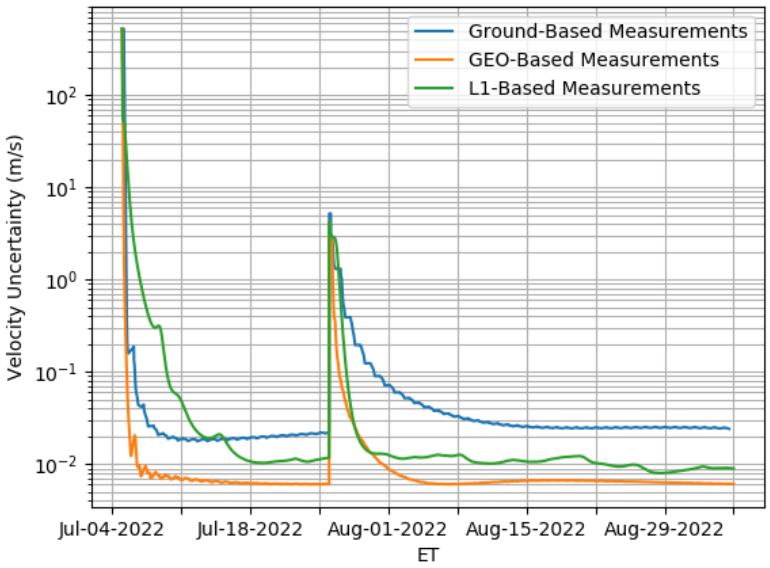


Fig. 12: Estimated velocity uncertainty (3-sigma) of low-energy transfer transmitter.

The results in this case are similar to previously studied cases, but there are some key differences. The GEO observers still provide the most accurate estimations, however for this transmitter trajectory, the L1-based observers perform better than the ground-based observers once the solution has converged to a steady-state uncertainty. The observers in L1 do require longer periods of time for the uncertainty to converge to the steady-state uncertainty however.

Conceptually, there is an understandable reason that the L1-based observers out-perform the ground-based observers for this case of a spacecraft well beyond the orbit of the Moon. As the Moon orbits the Earth, the interferometer at L1 moves with it, and observations are taken over time from a wide range of relative geometries. Compare this to the Earth observers, where the target transmitter moves very slowly with respect to Earth near apogee, and measurements over a period of many days provide essentially the same information content.

## 7. CONCLUSIONS

The analysis in this paper demonstrates the mathematical plausibility of space-based interferometry for estimating the state of RSOs that currently stress optical sensors. VLBI-based techniques have been used for cooperative orbit determination for decades, and in recent years have gained popularity as a supplementary technique to optical data for SDA in GEO and other orbit regimes. Extending ground-based interferometry into space allows for much longer baselines and ultimately better angular resolutions. Additionally, space-based receivers can provide additional viewing geometries over time, leading to better observability, faster convergence, and lower state uncertainties that ground-based receivers alone.

The case of an interferometer in GEO showed faster convergence than ground-based or libration point-based observers, and additionally showed better convergence than many similar test cases with space-based optical measurements that have been studied at the past. There are clear engineering challenges of space-based interferometers, but the mathematical and observability studies shown in this paper do demonstrate the potential usefulness of such a system given realistic test cases and simulated measurements.

## 8. ACKNOWLEDGEMENTS

All work presented here was fully funded via Advanced Space internal research and development funded. No government sponsorship or endorsement was provided or should be implied. The authors would like to thank Patrick Miga for helpful discussions on observability and information gain for XDA systems.

## 9. REFERENCES


[1] European Space Agency, “Space Debris by the Numbers,” 2022. .

[2] M. Bolden, T. Craychee, and E. Griggs, “An Evaluation of Observing Constellation Orbit Stability, Low Signal-to-Noise, and the Too-Short-Arc Challenges in the Cislunar Domain,” 2020.

[3] M. R. Thompson, N. P. Ré, C. Meek, and B. Cheetham, “Cislunar Orbit Determination and Tracking via Simulated Space-Based Measurements,” 2021.

[4] S. Knister, B. R. Williams, D. Hayhurst, K. W. Johnson, and B. D. Little, “Evaluation Framework for Cislunar Space Domain Awareness Systems,” 2021.

[5] E. E. Fowler, S. B. Hurtt, and D. A. Paley, “Orbit Design for Cislunar Space Domain Awareness,” 2020.

[6] K. A. Hill, “Autonomous Navigation in Libration Point Orbits,” University of Colorado, 2007.

[7] J. A. Greaves and D. J. Scheeres, “Relative Estimation in the Cislunar Regime using Optical Sensors,” 2021.

[8] J. K. Vendl and M. J. Holzinger, “Cislunar Periodic Orbit Analysis for Persistent Space Object Detection Capability,” 2020.

[9] M. Gupta, K. C. Howell, and C. Frueh, “Earth-Moon Multi-Body Orbit to Facilitate Cislunar Surveillance Activities,” 2021.

[10] C. Frueh, K. Howell, K. J. Demars, S. Bhadauria, and M. Gupta, “Cislunar Space Traffic Management: Surveillance Through Earth-Moon Resonance Orbits,” 2021.

[11] L. J. Wood, “The Evolution of Deep Space Navigation: 1962-1989,” *Adv. Astronaut. Sci.*, vol. 152, pp. 827–847, 2008.

[12] B. G. Lanyi, D. S. Bagri, and J. S. Border, “Angular Position Determination of Spacecraft by Radio Interferometry,” *Proc. IEEE*, vol. 95, no. 11, pp. 2193–2201, 2007.

[13] J. Border and J. Koukos, “Technical Characteristics and Accuracy Capabilities of Delta Differential One-Way Ranging (ΔDOR) as a Spacecraft Navigation Tool,” 1993.

[14] T. D. Moyer, “Formulation for Observed and Computed Values of Deep Space Network Data Types for Navigation,” *Deep Sp. Commun. Navig. Ser.*, 2005, doi: 10.1002/0471728470.

[15] K. Simon, “Passive RF in Support of Closely Spaced Objects Scenarios,” 2020.

[16] K. Simon, S. Williams, B. Sward, and A. Beer, “Space Object Identification, Discrimination, and Tracking,” 2021.

[17] D. A. Duev, G. Molera Calvés, S. V. Pogrebenko, L. I. Gurvits, G. Cimó, and T. Bocanegra Bahamon, “Spacecraft VLBI and Doppler Tracking: Algorithms and Implementation,” *Astron. Astrophys.*, vol. 541, pp. 1–9, 2012, doi: 10.1051/0004-6361/201218885.

[18] Y. Huang *et al.*, “Improvement of Orbit Determination for Geostationary Satellites with VLBI Tracking,” *Chinese Sci. Bull.*, vol. 56, no. 26, pp. 2765–2772, 2011, doi: 10.1007/s11434-011-4647-0.

[19] F. Fiori *et al.*, “Deep Space Orbit Determination via Delta-DOR Using VLBI Antennas,” *CEAS Sp. J.*, vol. 14, no. 2, pp. 421–430, 2022, doi: 10.1007/s12567-022-00424-5.

[20] D. L. Jones *et al.*, “Very Long Baseline Array Astrometric Observations of the Cassini Spacecraft at Saturn,” *Astron. J.*, vol. 141, no. 29, 2011, doi: 10.1088/0004-6256/141/2/29.

[21] W. Zheng *et al.*, “Real-time and High-Accuracy VLBI in the CE-3 Mission,” 2014.

[22] G. Klopotek *et al.*, “Position Determination of the Chang’e 3 Lander with Geodetic VLBI,” *Earth, Planets Sp.*, 2019, doi: 10.1186/s40623-019-1001-2.

[23] E. Wei *et al.*, “Simulation and Results on Real-Time Positioning of Chang’E-3 Rover with the Same-Beam VLBI Observations,” *Planet. Space Sci.*, vol. 84, pp. 20–27, 2013, doi: 10.1016/j.pss.2013.04.005.

[24] W. . Zhou *et al.*, “Tropospheric Delay Correction of VLBI Stations for the Real-Time Trajectory Determination of the Chang ’ E-5 Spacecraft,” *Radio Sci.*, vol. 57, 2022, doi: 10.1029/2022RS007440.

[25] H. Hanada *et al.*, “Overview of Differential VLBI Observations of Lunar Orbiters in SELENE (Kaguya) for Precise Orbit Determination and Lunar Gravity Field Study,” *Sp. Sci. Rev.*, vol. 154, pp. 123–144, 2010, doi: 10.1007/s11214-010-9656-9.

[26] M. Kaliuzhnyi *et al.*, “International Network of Passive Correlation Ranging for Orbit Determination of a Geostationary Satellite,” *Odessa Astron. Publ.*, vol. 29, pp. 203–206, 2016.

[27] N. Kinzly, B. Polzine, C. Short, and J. Woodburn, “Simulating a Dynamics-Informed Cislunar RPO Mission Incorporating Orbit Determin,” 2022.

[28] J. L. Geeraert and J. W. Mcmahon, “Relative Orbit Determination of Multiple Satellites Using Double Differenced Measurements,” 2017.

[29] J. L. Geeraert, “Multi-Satellite Orbit Determination Using Interferometric Observables with RF Localization Applications,” University of Colorado, 2017.

[30] L. I. Gurvits, “Space VLBI : From First Ideas to Operational Missions,” *Adv. Sp. Res.*, vol. 65, no. 2, pp. 868–876, 2020, doi: 10.1016/j.asr.2019.05.042.
[31] E. Wei *et al.*, “Contribution of Simulated Space VLBI to the Chang’E-1 Orbit Determination and EOPs Estimation,” *Aerosp. Sci. Technol.*, vol. 46, pp. 256–263, 2015, doi: 10.1016/j.ast.2015.07.016.
[32] D. W. Pesce *et al.*, “Extremely Long Baseline Interferometry with Origins Space Telescope,” 2019.
[33] P. Marzioli, F. Santoni, and F. Piergentili, “Evaluation of Time Difference of Arrival (TDOA) Networks Performance for Launcher Vehicles and Spacecraft Tracking,” *Aerospace*, vol. 7, no. 151, 2020.
[34] J. D. Bard and F. M. Ham, “Time Difference of Arrival Dilution of Precision and Applications,” *IEEE Trans. Signal Process.*, vol. 47, no. 2, pp. 521–523, 1999.
[35] M. V Shatskaya *et al.*, “Data Processing Center of RadioAstron Space VLBI Project,” *Adv. Sp. Res.*, vol. 65, no. 2, pp. 813–820, 2020, doi: 10.1016/j.asr.2019.05.043.
[36] M. V. Zakhvatkin *et al.*, “RadioAstron Orbit Determination and Evaluation of its Results Using Correlation of Space-VLBI Observations,” *Adv. Sp. Res.*, vol. 65, no. 2, pp. 798–812, 2020, doi: 10.1016/j.asr.2019.05.007.
[37] E. A. Burt *et al.*, “Demonstration of a Trapped-Ion Atomic Clock in Space,” *Nature*, vol. 595, no. 7865, pp. 43–47, 2021, doi: 10.1038/s41586-021-03571-7.
[38] T. Gardner *et al.*, “CAPSTONE: A Summary of Flight Operations to Date in the Cislunar Environment,” 2022.